Possible mechanism linking ocean conditions to low body weight and poor recruitment of age-0 walleye pollock (*Gadus chalcogrammus*) in the southeast Bering Sea during 2007

Jeanette C. Gann[a*], Lisa B. Eisner[b], Steve Porter[b], Jordan T. Watson[c], Kristin D. Cieciel[a], Calvin W. Mordy[d, e], Ellen M. Yasumiishi[a], Phyllis J. Stabeno[d], Carol Ladd[d], Ron A. Heintz[a], Edward V. Farley[a]

[a] NOAA-Fisheries, Alaska Fisheries Science Center/Auke Bay Laboratories, 17109 Pt. Lena Loop Road, Juneau, AK 99801, USA Jeanette.Gann@NOAA.gov, (001-907-789-6445); Kristin.Cieciel@NOAA.gov; Ellen.Yasumiishi@NOAA.gov; Ron.Heintz@NOAA.gov; Ed.Farley@NOAA.gov

[b] NOAA-Fisheries, Alaska Fisheries Science Center, 7600 Sand Point Way NE, Seattle, WA 98115, USA Lisa.Eisner@NOAA.gov; Steve.Porter@NOAA.gov

[c] University of Alaska Fairbanks, School of Fisheries and Ocean Sciences, 17109 Pt. Lena Loop Rd., Juneau, AK 99801, USA Jordan.Watson@NOAA.gov

[d] NOAA-Pacific Marine Environmental Laboratory, 7600 Sand Point Way, Seattle, WA 98115-6349, USA Phyllis.Stabeno@NOAA.gov; Carol.Ladd@NOAA.gov

[e] Joint Institute for the Study of the Atmosphere and Ocean, Box 355672, University of Washington, Seattle, WA 98105-5672 Calvin.W.Mordy@NOAA.gov

*Corresponding Author

Abstract

Changes to physical and chemical oceanographic structure can lead to changes in phytoplankton biomass and growth, which, in-turn, lead to variability in the amount of energy available for transfer to higher trophic levels (e.g. forage fish). In general, age-0 (juvenile) walleye pollock (*Gadus chalcogrammus*) have been shown to have low fitness (determined by energy density and size), in warm years compared to average or cold years in the southeastern Bering Sea. Contrary to these findings, the year 2007 was a cold year with low fitness of age-0 pollock compared to the transition year of 2006 (transitioning from warm to cold conditions) and cold years, 2008-2011. In late summer/early fall (mid-August through September), significantly lower surface silicic acid concentrations coupled with low phytoplankton production and chlorophyll *a* (Chl *a*) biomass were observed in 2007 among 2006-2012 ($P < 0.05$). We postulate that the low silicic acid concentrations may be an indication of reduced surface nutrient flux during summer leading to low primary productivity (PP). The nutrient replenishing shelf/slope water exchange that occurred during late October-February (2006-2007) indicates that deep water nutrient/salinity reserves for the start of the 2007 growing season, were plentiful and had similar concentrations to other years (2006-2012). The spring bloom magnitude appeared to be slightly below average, and surface silicic acid concentrations at the end of the spring bloom period in 2007 appeared similar to other years in the middle domain of the southeastern Bering Sea. However, during summer (June-August) 2007, high stratification and the low number of storm events resulted in low flux of nutrients to surface waters, indicated by the low surface silicic acid concentrations at the end of summer (mid-August through September). Surface silicic acid may be useful as an indicator of surface nutrient enrichment (and subsequent PP) during summer since other macronutrients (e.g. nitrate) are usually near or below detection limits at this time, and diatoms are generally scarce during summer. Surface silicic acid concentration was also positively associated with the size of juvenile fish (age-0 pollock weight and length). This reinforces the theory that nutrient availability and primary productivity are important to energy allocation for higher trophic levels during summer, and possibly provides links between stratification and wind mixing, surface nutrient input, PP and juvenile fish size and condition.

Keywords: *Gadus chalcogrammus*, primary productivity, silicic acid, nutrients, age-0, walleye pollock, juvenile, eastern Bering Sea

1. Introduction

Tracking the transfer of energy through an ecosystem from physics to fish can help us to better understand the ecosystem as a whole, and could eventually allow us to predict and consequently prepare for periods of low productivity. The timing, magnitude, and duration of seasonal primary productivity in subarctic coastal regions strongly influence the amount of energy as carbon that moves through the ecosystem (Sigler et al., this issue). This study focuses on the possible role of low silicic acid as an indicator of low summer primary productivity (PP) and low fitness (whole body energy content) of age-0 walleye pollock (*Gadus chalcogrammus*), hereafter referred to as pollock, in the eastern Bering Sea (EBS) during 2007.

The shelf of the EBS is an important rearing habitat for age-0 pollock (Coyle et al. 2011). The south EBS shelf is a broad shallow region that is oceanographically divided into three shelf domains based on depth: inner shelf (0-50 m), middle shelf (50-100 m) and outer shelf (100-200 m) with fronts that partition these domains and impede cross-shelf flow (Coachman, 1986; Kachel et al., 2002). Each domain displays specific oceanographic characteristics with a vertically well-mixed tidally influenced inner shelf, a stable 2-layer system over the middle shelf, and a 3-layer system with well mixed top and bottom layers over the outer shelf (Coachman, 1986). The entire EBS shelf is further divided by smaller spatial regions characterized by specific biological, oceanographic, and physical properties as defined for the Bering Sea Project (Bering Sea Ecosystem Study [BEST] and Bering Sea Integrated Ecosystem Research Program [BSIERP], Ortiz et al., 2012; Wiese et al., 2012). There are a total of seven regions that comprise the south EBS (south of ~ 60°N), the largest being Region 3, which covers a large portion of the south middle shelf (Ortiz et al., 2012).

Seasonal cycles of PP on the EBS shelf occur, with low (< 0.2 g C m^{-2} d^{-1}) winter values, relatively high rates (>1 g C m^{-2} d^{-1}) during the spring bloom typically peaking in May, low to moderate rates (0.2-0.6 g C m^{-2} d^{-1}) in summer with a mild (0.5-0.8 g C m^{-2} d^{-1}) fall bloom observed in some shelf regions (e.g. middle and inner shelf) (Brown et al., 2011; Rho and Whitledge, 2007). The spring bloom is initiated by increasing day length and shallowing of the mixed layer so that phytoplankton remain above the compensation depth and growth is no longer limited by light (Sverdrup, 1953). The availability of surface nutrients from mixing of the water

column over winter supports ice algae and phytoplankton blooms during spring, with large diatoms making up a high percentage of the biomass (Moran et al., 2012; Wyatt et al., 2013). As nutrients within the euphotic zone are exhausted, phytoplankton growth becomes nutrient limited and the spring bloom ends. Diatoms require nitrogen, phosphate and silicic acid for growth, however, nitrogen is usually the limiting nutrient, so residual silicic acid may remain in surface waters following the spring bloom. The size of the spring diatom bloom will, therefore, determine the amount of silicic acid remaining in the surface pool at the start of summer.

During summer, stratification in the water column restricts vertical movement of nutrients to the surface waters which reduces productivity and allows small phytoplankton taxa (e.g. microflagellates), favored under low nutrient conditions, to dominate the system (Moran et al., 2012). Depending on to the magnitude of wind events and the strength of water column stratification, episodic winds can break down stratification and mix nutrients into the euphotic zone, producing bouts of productivity during this period (Sambrotto et al., 1986; Stabeno et al., 2010). During these bouts of productivity, nitrate and ammonium are rapidly depleted by phytoplankton, again leaving residual silicic acid in surface waters. Hence, in summer if episodic mixing occurs, surface silicic acid is high; if no mixing occurs then silicic acid remains low.

The amount of carbon transferred from phytoplankton to higher tropic levels will be affected by the quantity of primary production and the size and quality of the individual phytoplankton taxa. Classically, larger-size phytoplankton taxa (e.g. diatoms) will result in shorter food webs leading to more efficient energy transfer (e.g. diatom to mesozooplantkon to fish) compared to smaller phytoplankton taxa (e.g. small flagellates to microzooplankton to mesozooplankton to fish) (Dahlgren et al., 2011). Therefore, higher nutrient conditions, as occur during episodic mixing events, can favor production of large taxa like diatoms, which may ultimately enhance carbon transfer to higher trophic levels, such as walleye pollock.

The health and survival of zooplankton and fish are tied to the timing of spring bloom and seasonal progression of productivity on the EBS shelf (Sigler et al., this issue). For example, the large copepod, *Calanus* spp., may depend upon early, ice-associated phytoplankton blooms or ice algae to avoid exhausting their over-wintering lipid reserves (Coyle et al., 2011) or for the successful recruitment of copepodites in spring (Baier and Napp, 2003). In the south EBS, warm years were characterized by low sea ice extent and cold years by high sea ice extent, and in recent decades, a stanza of low ice extent warm years (2001–2005), were followed by a

transition year (2006), and then a stanza of high ice extent cold years (2007-2013) (Stabeno et al., 2012; Zador, 2014). Recent years with anomalously warm temperatures in the south EBS were associated with lower abundances of large crustacean zooplankton and higher abundances of smaller zooplankton taxa (Coyle et al., 2011; Eisner et al., 2014). The shifts in zooplankton species assemblages were also associated with a shift in the prey of small pelagic fish (Coyle et al., 2011; Farley and Moss, 2009). Such changes led to a new conceptual model of carbon and energy flow during warm and cold years in the south EBS (Coyle et al., 2011) and to a revised oscillating control hypothesis connecting climate to recruitment of important groundfish populations (Hunt et al., 2011).

During their first year, fish vary how energy is allocated (either growth or storage) depending on their ontogenetic stage. During the larval phase (occurring in spring), energy is primarily allocated to somatic growth to help young larvae avoid predation. Once they reach >30 mm in length (considered age-0 or juveniles), energy is allocated to increase lipid storage which has important consequences for overwinter survival (Siddon et al., 2013). Mueter et al. (2011) developed a model for age-1 recruitment of pollock assuming that survival of early larvae are enhanced by warm spring conditions, but that high temperatures during late summer and autumn are associated with poor feeding conditions prior to winter and reduced recruitment in the following spring. This reinforces the importance of late summer/early fall conditions for overwinter survival for fish during the first year at sea.

The recent changes in zooplankton taxonomic composition (viewed as a proxy for prey quality) in the EBS had direct implications on age-0 pollock energy content and survival (Heintz et al., 2013). During warm years, age-0 (juvenile, fish that were hatched that same spring and have grown out of their larval stage) pollock that fed on smaller zooplankton taxa had significantly lower energy content than fish that fed on lipid-rich, large copepods and euphausiids during cold years (Heintz et al., 2013). Subsequently, the best model relating age-0 pollock fitness to their recruitment at age-1 included both size and energy content, indicating that both these variables are important for overwinter survival in the eastern Bering Sea (Heintz et al., 2013; Hunt et al., 2011). For example, collectively, age-0 pollock captured during 2007 had average energy density (lipid, kJ/g wet weight) but individually, were relatively small in size causing their whole body energy content (kJ/fish) to be low. Consequently, survival of age-0 pollock during winter 2007-2008 was low, even though they had attained average lipid reserves

during late summer and early fall (Heintz et al., 2013). Small size of age-0 Pacific cod (*Gadus macrocephalus*) during 2007 was also found (Farley et al., this issue) as well as reduced fitness of juvenile sockeye salmon (Farley et al., 2011).

The importance of stratification to juvenile pollock over-winter survival in the eastern Bering Sea also has been described by Coyle et al. (2011) who found a significant negative correlation between water column stratification during the first summer at sea (age-0 fish) and their survival to age-1. We propose that during years with high stratification and low wind mixing, low surface nutrient flux can result in a reduction in carbon transfer up the food web to fish, evidenced by reductions in the body size (due to slower growth) and fitness of age-0 pollock at the end of summer.

In this paper, we examine bottom-up conditions (e.g. nutrient availability, PP) during late summer/early fall for the years 2006 through 2012 to better understand the mechanisms that may have led to the reduced size and fitness of age-0 fish during 2007 in the south EBS, with an emphasis on oceanographic characteristics at PP stations and stations in the middle shelf Bering Sea Project Region 3. We used Region 3 for this analysis since there is a long record of oceanographic data in this region at the long-term Pacific marine Environmental Laboratory (PMEL) Mooring 2 (M2, 56.87°N, 164.06°W), and this region may be sensitive to surface nutrient depletion since it tends to be highly stratified during summer (Eisner et al., this issue; Ladd and Stabeno, 2012). Specifically, we examine silicic acid concentrations (as a proxy for nutrient input in summer), PP, pollock egg abundance and hatch timing, size of larval pollock, the size, diets, and energetic of age-0 pollock, and recruitment to age-1.

2. Methods

2.1 Data collection and sample analysis

2.1.1 Oceanographic data

Fisheries oceanography surveys were conducted on the south EBS shelf (south of 60°N) during mid-August through early October on Bering Arctic Sub-Arctic Integrated Survey (BASIS) cruises for 2006 to 2012 (described in Eisner et al., this issue). Hydrographic data (temperature, salinity, pressure, photosynthetically active radiation [PAR]), and water samples for chlorophyll *a* (Chl *a*) and nutrients (silicic acid, nitrate, ammonium, nitrite and phosphate)

were collected via Seabird Electronics CTD (9-11, or 25) equipped with auxiliary sensors, and a carousel housing Niskin bottles. Discrete Chl *a* samples (total from Whatman GF/F filters [0.7 µm] and >10 µm size fractions from polycarbonate membrane filters) were vacuum filtered and filters frozen at -80 ºC pending analysis using standard fluorometric methods (Parsons et al., 1984). Samples for nutrient analysis were frozen for later analysis following the WOCE-JGOFS standardization and analysis procedures specified by JGOFS (1994), including reagent preparation, calibration of labware, preparation of primary and secondary standards, and corrections for blanks and refractive index. Vertical profiles of PAR were obtained from Li-Cor or Bio-Spherical 4 pi sensors mounted on the CTD, and above surface PAR was measured with Li-Cor or Hobo 2 pi sensors.

Shipboard PP experiments were conducted to estimate rates of carbon uptake by phytoplankton. Samples for PP experiments were collected from 50% down to 1% of surface light level (estimated using a biospherical PAR sensor attached to the CTD) with two light bottles (duplicates) and one dark bottle collected at each sample depth. Experiments were conducted at a subset of stations in 2006–2011 (excluding 2008), for a total of 32 stations (Fig. 1). We used 500 ml clear polycarbonate bottles filled with surface water (collected ~ mid-morning) and inoculated with 7.5 x 10^5 moles L^{-1} $NaH_{13}CO_3$. Control samples (without inoculation) were filtered immediately onto pre-combusted Whatman GF/F filters, while the remaining inoculated bottles were placed in screen bags that simulated 50% down to 1% light levels and incubated for six hours approximately centered over local solar noon in deck-board acrylic glass tanks cooled with surface seawater. After incubation, samples were filtered onto Whatman GF/F filters and were frozen at -80°C. Samples were analyzed within 6 months at the University of Alaska Fairbanks (UAF) Stable Isotope Facility using a Delta V continuous-flow isotope ratio mass spectrometer interfaced with a Costech ESC 4010 elemental analyzer.

PP data were obtained from UAF as del ^{13}C values ($\delta^{13}C$ PDB ‰) and as carbon mass (µg). Data were converted to atom percent (AP) using the equation:

$$AP = 100*((AR*(\delta^{13}C/1000) +1) / (1+AR*(\delta^{13}C/1000)) + 1$$

Where AR, the absolute ratio, is a constant equal to 0.112 and $\delta^{13}C$ is the value in 'per mil' (‰) obtained by the lab (equation from the University of Ottawa stable isotope laboratory and 'A

206 Guide to the Calculation of Isotope Ratios' Europa Scientific LTD). A dissolved fraction for
207 atom percent (APD) was calculated as:

208 $$APD = ((C^{13})/ TCO_2)/(1+ C^{13} \text{ addition})/ TCO_2))*100$$

209 Where C^{13} = the carbon-13 experimental addition, and TCO_2 is the total dissolved carbon dioxide
210 value (mmol/L). The APD and both pre and post incubation atom percent values were used to
211 obtain an uptake rate via the equation:

212 $$\text{Uptake } (\mu g\ L^{-1} \text{ experiment}^{-1}) = \text{Carbon Mass } (\mu g)*((APP - AP)/(APD-AP))$$

213 Where APP = atom percent post incubation, and AP is the pre-incubation atom percent. Uptake
214 rates were then converted to mg m^{-3} hr^{-1} by dividing uptake per experiment by the incubation
215 time (as per Hama et al., 1983).
216 Science quality monthly average Chl *a* (mg m^{-3}) data from the Moderate Resolution Imaging
217 Spectroradiometer (MODIS) were downloaded from NOAA's CoastWatch program
218 (http://coastwatch.pfeg.noaa.gov/infog/MH_chla_las.html). NASA's Goddard Space Flight
219 Center (GSFC) receives raw satellite data. The SeaWiFS Data Analysis System (SeaDAS)
220 software (Fu et al., 1998) is used to process the raw data. An atmospheric correction is applied to
221 yield water leaving radiance (Gordon and Wang, 1994; Shettle and Fenn, 1979) which is then
222 processed to Chl *a* using the NASA developed OC3M algorithm (O'Reilly et al., 2000).

223 *2.1.2 Spring ichthyoplankton*

224 Pollock larval standard length comparisons and egg abundance were examined during
225 springtime ichthyoplankton surveys in the south EBS from 2006 to 2012. Gear used for sampling
226 were a 60 cm Bongo array or a 1-m^2 Multiple Opening/Closing Net Environmental Sensing
227 System (MOCNESS) with either 333 or 505 µm mesh nets, and catch was integrated over the
228 water column. Egg abundance analysis was performed for the years 2006 to 2010, and 2012, and
229 only stations where eggs were present were analyzed. Those stations were located mostly along
230 the Alaska Peninsula and near the Pribilof Islands (Fig. 1). Pollock spawn at different times and
231 at different locations in the Bering Sea (Bacheler et al., 2010) and comparing different locations
232 could complicate interpreting larval size differences. Based on the number of stations surveyed

and the spatial coverage, annual pollock larval size comparisons were thus performed using the Pribilof Islands spawning area (for years 2007, 2009, 2010, and 2012).

2.1.3 Late summer age-0 pollock size, diet, and energy

All age-0 pollock were collected concurrently with oceanographic data. Pelagic fish were collected using a can-trawl net, 198 m long, with a hexagonal mesh in wings and body, and a 1.2 cm mesh liner in the cod-end. The trawl was towed at 6.5-9.3 km h^{-1}, at or near the surface, and had a typical spread of 55 m horizontally and 25 m vertically. Trawl stations were sampled during daylight, and all tows lasted 30 min and covered 2.8-4.6 km. A total of 701,139 age-0s were caught over the south EBS shelf for 2006-2012, largely over the inner and middle domains. A subsample of up to 50 age-0 pollock (< 101 mm) were weighed in bulk at each station. Bulk subsample weights for each station were divided by the number of fish within the subsample for use as a catch-averaged weight/station (A0W). The lowest number of fish measured in any given year occurred in 2009 where 995 age-0 pollock were caught.

Food habits of age-0 pollock were examined onboard each vessel during BASIS late summer/early fall surveys by removing and pooling the contents of the entire food bolus from the stomachs of up to 20 randomly selected individuals. Stomach contents were weighed to the nearest 0.001 g, sorted, and identified to the lowest feasible taxonomic group. Individual prey groups were weighed (wet weights) and divided by the total weight of prey contained in the stomachs to calculate proportional contributions of each prey group to the diet. In cases where prey categories were too small to weigh individually, an estimate was made of its percent contribution. Data from 2006-2009 are presented in Moss et al. (2009) and Coyle et al. (2011). New data for this manuscript includes 2010-2012. A stomach fullness index also was calculated aboard ship by first calculating a stomach content index (SCI) dividing each prey category (identified to the lowest feasible taxonomic group) by the weight of each fish and multiplying by 10,000. All individual prey SCI's then sum up to the stomach fullness index.

Energetics (energy content) data of age-0 pollock are from Heintz et al. (2013). The year 2012 was added to the data for reproduction in this manuscript. Methods for lipid analysis can be found in Heintz et al. (2013).

2.2 Data analysis and statistics

262 *2.2.1 Oceanographic data*

263 Interannual comparisons (2006-2012) of late summer/early fall surface and bottom
264 temperature, and mixed layer depth were conducted using Region 3 stations that were sampled a
265 minimum of 5 of the years during 2006-2012. The mixed layer depth and surface and bottom
266 temperatures (°C, mean above and below the mixed layer depth) were derived from CTD profile
267 data (Danielson et al., 2011; Eisner et al., this issue). We also conducted comparisons of surface
268 Chl *a* (mg m^{-3}, total and large size fraction [>10 µm Chl *a*]) and silicic acid ($Si(OH)_4$, µM) on
269 data from PP stations and on data collected in Region 3. Surface silicic acid, surface Chl *a*, and
270 surface large size fraction Chl *a* were natural log transformed, and one way ANOVA tests were
271 performed to examine means among years. A Student Neuman-Keuls test using R with the
272 agricolae package (version 3.0.1, The R Foundation for Statistical Computing; R Core Team,
273 2013) was used for pairwise comparisons to illustrate significant differences between pairs of
274 years. On-way ANOVA was used to determine differences for silicic acid concentrations
275 (untransformed) below the pycnocline (30-60 m) in Region 3.

276 Interannual differences in late summer/early fall PP were investigated for 2006-2011
277 (excluding 2008) at PP stations located on the inner and middle south EBS shelf (Fig. 1). PP data
278 was evaluated for absolute uptake rates (mg C m^{-3} hr^{-1}), normalized by Chl *a* (mg C mg Chl a^{-1}
279 hr^{-1}), and further normalized by PAR (mg C mg Chl a^{-1} hr^{-1} µmol $photons^{-1}$ m^{-2} s^{-1}), to assess
280 effects of biomass and light on uptake rates. Duplicate light bottle samples with a high (> 50)
281 coefficient of variation (CV, sample standard deviation/mean) were not used for the analysis
282 Data for PP were not normally distributed even after log transformation. Sample size was also
283 relatively small so we used a non-parametric Kruskal-Wallis rank sum analysis to determine
284 significant interannual variations in PP.

285 MODIS ocean color data from Region 3 were used to investigate seasonal and interannual
286 variations in Chl *a*. Mean and standard errors were calculated for Chl *a* (mg m^{-3}) for March-May
287 (spring), June-Aug (summer), September-October (fall), and March-August (an indicator of Chla
288 biomass in spring and summer prior to our survey). One-way ANOVA was used to determine
289 significant differences. Maximum Chl *a* values for autumn and spring months were determined
290 for each year (2006-2012), and average monthly Chl *a* values from spring to fall (April-October)
291 were compared graphically. We further characterized spring bloom magnitude and estimated
292 post bloom surface silicic acid at M2 using data from PMEL hydrographic surveys and BEST

surveys (Wiese et al., 2012). Silicic acid was analyzed by PMEL following similar methods as described above for BASIS surveys (Mordy et al., 2012). We evaluated the date and magnitude of the spring bloom maximum using surface Chl *a* fluorescence data from moored sensors (reproduced from Sigler et al., 2014), and estimated the date and magnitude of post bloom surface silicic acid (for a subset of years: 2007, 2009, 2010) from discrete water samples. One-way ANOVA was used to determine if post-bloom surface silicic acid varied among years.

2.2.2 Oceanography and age-0 pollock size comparisons

Oceanographic discrete sample data (silicic acid and Chl *a*) from Region 3, were compared with age-0 pollock weights (weighted means/station/year) south of 60 ºN latitude. To enhance visual comparisons among variables, silicic acid, Chl *a*, and A0W values were normalized for time series plots by subtracting the mean (2006-2012) from each value and dividing by the standard deviation. Pearson's product correlations were used to evaluate linear relationships between yearly mean surface silicic acid, surface Chl *a*, integrated Chl *a* (mg m^{-2}), and A0W (g) for 2006-2012. One-way ANOVA was used to compare A0W among years

2.2.3 Spring ichthyoplankton

Pollock egg abundance varies spatially on a daily scale because pollock spawn at separate times and locations throughout the Bering Sea. Spatial coverage was not equal among years so a variable coefficient Generalized Additive Model (GAM) was used (R package mgcv, version 1.7-22; Wood, 2006) to estimate date of peak egg abundance for each year based on day of year, longitude, and latitude. The response variable was number of eggs per 10 m^2 (log transformed), with longitude and latitude used as smooth terms. Models were analyzed in R. A mixed-effects ANOVA and Tukey's Test were used for larval size comparisons among years. The random effect for the ANOVA was station (a plankton tow conducted at a specific location), and Systat version 13.0 statistical software was used to run the analysis.

2.2.4 Age-0 pollock diets and energy

A linear regression model was used to relate the total body energy (KJ/fish) of age-0 pollock in year *t*-1 to subsequent recruitment to age-1 in year *t*.

3. Results

321 *3.1 Oceanographic data*

322 Surface temperatures in Region 3 (2006-2012) during August-September were highest during
323 2007, with a shallower mixed layer depth than other years studied (Table 1). Comparisons
324 among PP stations (and Region 3 stations in years without PP data, e.g. 2008, 2012) in late
325 summer /early fall indicate that the lowest mean Chl *a* biomass occurred in 2007, with
326 significantly lower values found in 2007 than 2009 and 2011 (Fig. 2, Table 2). The large (>10
327 µm) Chl *a* size fraction had the lowest values in 2007, 2008 and 2012, with significant different
328 ($P < 0.05$) observed between: 2007 vs 2009, 2008 vs 2009 and 2012 vs 2006, 2009, 2011 (Fig. 2,
329 Table 2). The mean and standard deviation (SD) for the total and large size fraction Chl *a*, all
330 years combined, was 1.43 (SD = 0.50) and 0.23 (SD = 0.22) mg m^{-3}, respectively.
331 Mean surface Chl *a* values (mg m^{-3}) derived from the aqua MODIS ocean color data in
332 Region 3 over the growing season during 2006-2012, indicate that 2007 had an early (April)
333 spring bloom with slightly below average values observed during all seasons (Table 3, Fig. 3).
334 However, no significant interannual differences among years could be detected (Table 3,
335 ANOVA, $P > 0.3$). Chl *a* fluorescence data at M2 collaborate these observations on bloom
336 timing and magnitude (Table 4). The maximum Chl *a* concentration during spring 2007 was 9.2
337 mg m^{-3}compared to a mean of 16.9 (SE = 2.9) for 2006-2011 (Table 4). Similar results (data not
338 shown) were estimated for PMEL Mooring 4 (M4), located at 57.9°N, 168.9°W, in the middle
339 domain inshore of the Pribilof Islands; 2007 had a mean of 10.6 mg m^{-3} compared to a mean of
340 20.1 (SE = 9.7) for 2006-2009 and 2011, (Sigler et al. 2014).
341 Surface silicic acid concentrations were significantly lower ($P < 0.05$) during late
342 summer/early fall 2007 compared to all other years examined in Region 3 and at PP stations
343 (Table 2, Fig. 2.). In addition, silicic acid values were lower, and dissolved inorganic nitrogen:
344 silicic acid (N: Si) ratios were higher in Region 3 compared to other areas of the EBS (with the
345 exception of the south inner shelf) during late summer 2007 (Fig. 4). This was also the area with
346 lowest PP in 2007 (data not shown). There was a significantly positive ($P < 0.05$) correlation
347 between surface silicic acid and surface in situ Chl *a* (Fig. 5A and Table 5). Concentrations for
348 silicic acid below the pycnocline (30-60 m) were evaluated for the years 2006-2012 (Fig. 6) and
349 appeared to be neither limiting for diatom growth, nor significantly different across all years,
350 with the exception of 2011 which was higher than all other years ($P < 0.05$, ANOVA).

Surface silicic acid concentrations (averaged over top 10 m) at M2 were measured 2-3 weeks after the maximum Chl *a* spring bloom peak for 2007, 2009 and 2010 (Table 4). Analysis of this (limited) data set, indicated that post bloom surface silicic acid concentrations were low (0.1-1.2 µM, Table 4) and similar among years (ANOVA, $P = 0.3$).

There were significant interannual differences ($P < 0.05$) in surface PP, PP normalized to Chl *a*, and PP normalized to both Chl *a* and PAR (Table 2). Overall, the lowest mean and median values for surface PP, surface silicic acid, and surface Chl *a* were observed in 2007 (Fig. 2). Integrated and surface PP uptake rates (uptake C, µg L^{-1}, h^{-1}) were significantly positively related ($R^2 = 0.70$, $P < 0.001$) (Fig. 7).

3.2 Oceanography and pollock size comparisons

Similar trends were observed for silicic acid and A0W from 2006 to 2012 (Fig. 5B, C). Surface silicic acid and A0W (and age-0 length data, not shown) did not have significant correlations for 2006-2012 ($P > 0.05$, Table 5). However, a linear trend is suggested for silicic acid values below 6 µM (Fig. 5C), suggesting a possible threshold response of A0W to silicic acid. Reanalysis of this data after removal of the 2011 high silicic acid data point, yielded higher correlations ($R = 0.77$, $P = 0.07$). The smallest (2007 and 2012) age-0 pollock were about half the mean size of the largest (2008 and 2009) fish (Fig. 8), however, no significant ($P > 0.05$) interannual differences were detected.

3.3 Spring ichthyoplankton

Peak egg abundance occurred in late April in 2006, mid-May from 2007-2010, and late May in 2012 (Table 6). Pollock eggs on the Bering Sea shelf are located in the upper 30 m of the water column (Smart et al., 2013), so sea surface temperature can be used as a proxy for temperature that eggs experience during development. Given the temperatures that occurred in 2007 to 2010, eggs would reach the hatching stage in approximately 32 to 36 days (Blood, 2002; Table 7). Duration of the hatching period (the time it takes for all eggs to hatch) is about 11 days for temperatures between 0.4 and 2.0 ºC (Blood, 2002). Given that peak egg abundance occurred near mid-May, the times to 50% hatching were alike, and there was an extended hatching period; it is likely that a portion of the eggs spawned during 2007 to 2010 hatched on similar dates (Table 7). For ichthyoplankton data during 2012, the coldest year, temperature appeared to have

the strongest effect on date of peak egg abundance (according to the GAM), resulting in the peak occurring 2 weeks later than in other years (Table 6).

Pollock larvae standard lengths were significantly different among years ($P < 0.001$, Table 8). Larvae collected in 2007 were significantly larger than larvae from 2009 and 2010 (all larvae were sampled near the middle of May, Table 8). There was no significant difference in size between 2007 and 2012 larvae, but 2012 larvae were collected about two weeks later than all other years and that may have influenced their size (Table 8). Alternatively, both spawning and hatching may have occurred later in 2012 due to the cold water temperature; in that case larvae from both years would be of similar age and size. Larvae in 2007 were larger than those in 2009 and 2010, but as age-0's were considered small (by weight; Figs. 5B, 8).

3.4 Age-0 pollock diets and energy

Diets of age-0 pollock varied among years 2006-2012 (Fig. 9). Age-0 diets in 2006 and 2007 were highly varied with the large copepod, *Calanus* spp., making up a smaller portion of diets compared with later years. The euphausiid, *Thysanoessa raschii*, and *Calanus* spp. made up the largest portions of age-0 diets during 2007 (26.9% and 20.5% respectively), while in other years (except for 2009), *Calanus* spp. alone accounted for the largest portion of diets, especially in 2012 (60%). The percentages of large crustacean zooplankton (lipid rich taxa, primarily *Calanus* spp., and euphausiids) were ~ 40% in 2006, 2007 and 2009, with percentages almost twice as high (~ 75%) in other years The stomach fullness index for age-0 pollock was similar among years with the exception of 2011 which was significantly lower ($P < 0.05$) than all other years (data not shown).

A regression of age-0 pollock fitness (kJ/fish) against age-1 recruitment (age-0 survivors quantified the following spring) for 2003-2012 indicates most cold and average years have good overwinter survival compared with poor survival during warm years and during 2007, with the exception of 2012 which had good survival to age-1, but poor fitness at the time of collection (Fig. 10).

4. Discussion

The goal of this study was to identify anomalous conditions in the south EBS for the year 2007 (within 2006-2012), that point to low energy transfer up the food web from physics to

juvenile fish during summer. We focused on summer surface silicic acid concentration as an indicator of summer PP; and the potential relationship of this indicator to size, fitness and over-winter survival of age-0 pollock. Here we discuss: 1) silicic acid concentrations, PP and Chl *a* biomass, 2) zooplankton and age-0 pollock feeding habits; 3) age-0 pollock size and fitness; 4) links between silicic acid and age-0 pollock that illustrate the importance of summer PP on juvenile forage fish (age-0) survival in their first year of life.

4.1 Silicic acid, PP and Chl a biomass

In order to evaluate the factors driving silicic acid concentrations in late summer (and its potential as an indicator of summer PP), we evaluated winter nutrient replenishment, and draw down during the spring bloom prior to the summer period, and episodic mixing events over the summer period.

The southern shelf water of the EBS is exchanged with slope water during October–January every year. On the middle shelf, this replenishes ~ 50% of the nutrients consumed during the previous season, although the extent of replenishment varies each year (Granger et al., 2013; Stabeno et al., this issue). Replenishment during fall and winter 2006/2007 was typical (~ 50%), likely providing an average nutrient pool (average silicic acid concentrations) for the start of the 2007 spring bloom (Stabeno et al., this issue).

The concentration of post-spring bloom surface silicic acid was also likely similar in 2007 compared to other study years. Nitrate in the upper mixed layer is depleted while ammonium concentrations increase in the bottom layer (Mordy et al., 2012). Surface silicic acid concentrations after the spring bloom were similar and low (mean < 1 μM) for 2007, 2009 and 2010 near M2. The spring diatom also did not appear to be higher in 2007 than other years based on Chl *a* fluorescence data at mooring M2 and M4 (Table 4, Sigler et al., 2014). MODIS Chl *a* data (Fig. 3) in Region 3 also suggest that the spring phytoplankton bloom was not exceptionally high in 2007; although ice algae and under ice or subsurface blooms cannot be evaluated with these satellite observations. Comparisons among years 2006-2011 show an earlier peak (April) in Chl *a* fluorescence data at M2 for 2007 (Table 4, Sigler et al., 2014), which agrees with satellite data, albeit 2012 also had an early peak. Since surface nutrients are consumed during the spring bloom, 2007 may have had a longer period of low surface nutrients than other years (starting in April instead of May), with the exception of 2012.

During summer, stratification and wind mixing can play a large part in regulating surface nutrient flux and PP over the southern EBS shelf (Sambrotto et al., 1986). At M2 there was very strong stratification and little to no mixing from June through August 2007 (Ladd and Stabeno, 2012; Stabeno et al., 2012). The years 2004 and 2007 had the highest stratification index values within 2003-2012 at M2 over the south middle shelf, with the lowest number of wind mixing events occurring in 2007 (3 events compared to a mean of 8, Eisner et al., this issue). The low surface silicic acid concentrations observed mid-August to September in 2007 support the conclusion that low episodic mixing in summer may have reduced the total surface nutrient flux during summer. The 2007 surface silicic acid concentrations were also unusually low when values are compared across a larger data set (Eisner et al., this issue). Values for Region 3 and the south inner shelf (Regions 2 and 7, Fig. 1) in 2007 were 1.6-1.9 µM compared to the means for 2003-2012 (4.2-4.8 µM) (Eisner et al., this issue). The only other mean values less than 2 µM for 2003-2012 were seen in the south inner shelf during 2011 and 2005. Region 3 has the strongest stratification over the south EBS (Ladd and Stabeno, 2012), so we may naturally expect nutrient limitation to be the highest in this region. The silicic acid concentrations below the pycnocline in 2007 were near average for Region 3 (Fig. 6, 23.8 for 2007 compared to 22.2 µM for 2003-2012; Eisner et al., this issue). However, the high stratification and low number of wind mixing events in 2007 did not allow those nutrients to mix to the surface. The low to moderate MODIS Chla data observed during the summer of 2007 suggests that low mixing rather than surface diatom PP prior to our survey was responsible for the observed low surface silicic acid values.

Late summer surface PP varied directly with Chl *a* biomass for cold years over the southeastern middle shelf from 2006 to 2012 (Fig. 2A, C). The significantly lower surface PP (absolute uptake) and Chl *a* biomass in 2007 compared to other years suggests that reduction in overall carbon uptake rates may be, in part, related to lower phytoplankton biomass. This is further supported by the findings of Brown et al. (2011), showing that Chl *a* and PP have a positive relationship on the EBS shelf. We also found in situ integrated PP and surface PP to be significantly positively related in the south EBS, as observed by Lomas et al. (2012). This suggests that water column PP was also low in 2007. A negative anomaly was observed for integrated Chl *a* (collected concurrently with surface PP and Chl *a* in the current study) solely during 2007 even within the larger span of 2003-2012 over the south middle shelf in Region 3

(Eisner et al., this issue), indicating that in 2007 Chl *a* biomass as well as PP were low throughout the water column.

The significantly low surface silicic acid (< 2 µM) in mid-August to mid-September in 2007 could also have altered phytoplankton community composition. A laboratory experimental study by Egge and Aksnes (1992) revealed that that when silicic acid concentrations were > 2 µM, phytoplankton communities may be diatom-dominated provided sufficient nitrogen is present. When concentrations were < 2 µM, diatom abundance was shown to decrease considerably regardless of nitrogen and phosphate supplies. The low amount of Chl *a* in the large fraction biomass (> 10 µm Chl *a*) in 2007 supports the conclusion that fewer diatoms were present in surface waters in 2007 than in most other years and that diatom PP was limited. Integrated (over top 50 m) large fraction Chl *a* in Region 3 was low in 2007 and 2008, but not in 2012 (Eisner et al., this issue). This discrepancy suggests that in 2012 taxa size may have varied considerably from surface to depth with large phytoplankton taxa (e.g. diatoms) located deeper in the water column.

4.2 Zooplankton and age-0 pollock feeding habits

Variations in availability and health of zooplankton prey during summer can have large impacts on age-0 pollock feeding. A considerably larger percentage of *Calanus* spp. was consumed as part of age-0 late summer diets during 2008-2012 as opposed to 2006-2007, when large zooplankton abundance was relatively low (Coyle et al., 2011, Eisner et al., 2014). The warm years ended in 2005; subsequently, *Calanus* spp. biomass increased starting in 2007 but had the greatest increase in 2008 indicating the potential for a considerable lag time for increases in large lipid-rich zooplankton from warm to cold years (Eisner et al., 2014). Zooplankton biomass in late summer of 2007 was also lower than 2008-2010, but not as low as 2003-2006 (Eisner et al., 2014; Eisner pers. comm.).

The higher surface temperatures in 2007 could also have increased energy expenditures by zooplankton (Coyle et al., 2011; Sigler et al., 2014). High energy expenditures and potentially lower availability of energy resources (due to lower summer PP, reflected by lower silicic acid concentrations) in 2007, could have led to reduced health of zooplankton prey (and a less nutritious food source for higher trophic levels). The low availability of diatom prey, potentially

499 high quality food for copepods (Vargas et al., 2010), also could have adversely affected *Calanus*
500 spp. growth and survival.

501 *4.3 Age-0 pollock* size and fitness

502 Age-0 pollock captured during late summer (2003-2011) in the south EBS had significantly
503 lower energy density (KJ/g) during warm years (2003-2005) compared to cold years (2007-2011)
504 (Heintz et al., 2013; Moss et al., 2009). Both cold years 2007 and 2012, age-0 pollock had low
505 total body energy content (kJ/fish), similar to that of warm years (Heintz et al., 2013). However,
506 overwinter survival of age-0's were low during 2007, but high during 2012. The 2012 year class
507 also appears to be strong based on acoustic surveys during 2014 (Ianelli et al., 2014). High total
508 surface Chl *a*, high abundance of large copepods and euphausiids in diets, and low temperatures
509 may have helped the 2012 age-0's to increase their lipid reserves during the time between our
510 survey and the onset of winter, considering that lower water temperatures can reduce metabolic
511 costs in fish, similar to zooplankton (Sigler et al., this issue). These oceanographic factors may
512 have aided lipid storage for juvenile fish during the cold summer of 2012, and impeded it during
513 the warm summer of 2007. Egg hatch timing was~2 weeks later in 2012 than in 2007, suggesting
514 that although the 2007 and 2012 age-0 fish were of similar size at the end of summer, the 2012
515 fish may have been younger and hence grown faster than the 2007 fish. Egg hatch times among
516 2007-2010 were similar, though larval sizes were in fact larger during 2007 than in 2009 and
517 2010. Accordingly, growth may have been faster in 2009 and 2010 because larvae were smaller
518 but juveniles were larger than those from 2007. Likewise, surface silicic acid concentrations
519 were higher in 2009 and 2010 than in 2007. This supports the hypothesis that the small size of
520 juvenile age-0 pollock in late summer/early fall 2007 was due to limited growth during the
521 summer as opposed to late hatching or small larval size in spring. It should be noted that the
522 larvae analyzed were not from the area shown to have low silicic acid levels.
523 Wind mixing and stratification may also directly affect fitness of age-0 pollock by affecting
524 the predator-prey interactions of larval and age-0 fish in the upper water column. Typical fish
525 feeding is analyzed by looking at the process of encounter, pursuit, attack and capture (Holling,
526 1959; Rothschild and Osborn, 1988). Higher predator-prey encounter rates will ultimately lead to
527 more chances for pursuit and capture of prey. MacKenzie et al. (1994) found evidence of a dome
528 shaped relationship between turbulence and larval fish-prey interactions, where rates of larval

529 fish ingestion increased with higher turbulence (i.e. more water column mixing and lower
530 stratification). Once a certain amount of turbulence was reached and surpassed, ingestion rates
531 fell again. This indicates that there could be an optimal range for water column stratification
532 where age-0 pollock increase their chances for prey encounters, without their foraging success
533 being compromised by high turbulence. Evidence for this dome-shaped relationship has also
534 been found by Mueter et al. (2006), specifically between age-0 pollock (log-survival) and wind
535 mixing, which is related to stratification.

536 *4.4 Links between surface silicic acid, PP and fish*

537 A nonlinear relationship was observed between surface silicic acid and the body weight of
538 age-0 pollock in September for years from 2006 to 2012 (Fig. 5C). A possible saturation
539 response may be proposed from a plot of A0W vs. silicic acid, with a significant linear trend
540 observed for silicic acid values less than ~6 μM, though additional data are needed in order to
541 verify this relationship. This suggests that increases in nutrient flux and subsequently summer PP
542 above a threshold level may provide more food (production) than needed for age-0 pollock
543 growth. These results suggest a possible link between age-0 pollock condition during late
544 summer, nutrient input and PP. The importance of lipid storage and growth for juvenile fish that
545 occurs during the long period of summer and fall could ultimately be responsible for their
546 overwinter survival (Coyle et al., 2011; Siddon et al., 2013; Sigler et al., this issue). Therefore,
547 2007 stands out as an anomalous year in the south EBS for fitness of age-0 and other juvenile
548 fish (Farley et al., this issue) among years with colder spring and summer water temperatures.

549 **5. Summary**

550 Oceanographic conditions and phytoplankton productivity throughout the growing season in
551 the south EBS may help to explain interannual variations in ecosystem dynamics and forage fish
552 condition as winter approaches. The year 2007 stands out as an example of anomalous conditions
553 (within average and cold years), where we see the importance of summer oceanographic
554 conditions and nutrient availability on production and biomass of phytoplankton, and transfer of
555 energy up the food web. Spring conditions play an important role in the setup of energy-rich
556 large crustacean zooplankton communities that ultimately provide for increased growth and lipid
557 storage in juvenile fish during summer (Sigler et al., this issue). However, summer PP is also

558 required to sustain zooplankton growth over the growing season. The year 2007 appeared to have
559 a good spring setup, with southerly ice extent likely providing an early food source of ice algae
560 or phytoplankton (Baeir and Napp, 2003). However, in summer, reduced mixing, likely led to
561 low surface nutrient flux, indicated by low levels of silicic acid and low PP. Low phytoplankton
562 production during summer, in addition to high surface temperatures (increasing metabolic
563 demands) may have reduced the health and abundance of large zooplankton (e.g. Calanus spp.
564 had lower biomass [Eisner et al., 2014] and contributed less to age-0 pollock diets in 2007 than
565 in most later years), and led to smaller less energy-rich fish just prior to winter.

566 **Acknowledgments**

567 We thank the captains and crews of the NOAA ship *Oscar Dyson*, and charter vessels, *Sea*
568 *Storm*, *NW Explorer*, and *Epic Explorer* and *Bristol Explorer* for many years of sampling. We
569 thank Natalia Kuznetsova and Mary Auburn-Cook for processing age-0 walleye pollock diet
570 samples. We are very grateful for the assistance in field sampling, data processing and analysis
571 of oceanographic and fisheries data from NOAA scientific staff and volunteers. In particular we
572 thank A. Andrews, M. Courtney, A. Feldman, J. Murphy, and W. Strasburger for their years of
573 survey participation. We'd also like to thank P. Proctor and E. Wisegarver for nutrient analysis,
574 and Mike Sigler for allowing us to reproduce data from Sigler et al., 2014. We acknowledge the
575 NOAA CoastWatch Program and NASA's Goddard Space Flight Center, OceanColor Web for
576 MODIS ocean color data. Funding was provided by National Science North Pacific Research
577 Board, Bering Sea Fisherman's Association, Arctic-Yukon-Kuskokwim-Sustainable-Salmon-
578 Initiative, the National Science Foundation (grants 1107250), and NOAA National Marine
579 Fisheries Service including the Fisheries and the Environment (FATE) programs. This
580 publication was partially funded by the Joint Institute for the Study of the Atmosphere and
581 Ocean (JISAO) under NOAA Cooperative Agreements NA17RJ1232 and NA10OAR4320148,
582 and is contribution 0823 to NOAA's Ecosystems and Fisheries-Oceanography Coordinated
583 Investigations, contribution 2255 to JISAO, contribution 4165 to NOAA's Pacific Marine
584 Environmental Laboratory, and BEST-BSIERP publication number XX. The findings and
585 conclusions in this paper are those of the authors and do not necessarily represent the views of
586 NOAA's Oceans and Atmospheric Research.

587

588 **References**

589 Bacheler N.M., Ciannelli L., Bailey K.M., Duffy-Anderson J.T., 2010. Spatial and temporal
590 patterns of walleye pollock (*Theragra chalcogramma*) spawning in the eastern Bering
591 Sea inferred from egg and larval distributions. Fish. Ocean. 19, 107-120.
592
593 Baier, C.T., Napp, J.M., 2003. Climate-induced variability in *Calanus marshallae* populations. J.
594 Plankton Res. 25, 771-782.
595
596 Blood, D.M. 2002. Low-temperature incubation of walleye pollock (Theragra chalcogramma)
597 eggs from the southeast Bering Sea shelf and Shelikof Strait, Gulf of Alaska. Deep-Sea
598 Research II 49, 6095-6108.
599
600 Brown, Z.W., van Dijken, G.L., Arrigo, K.R., 2011. A reassessment of primary production and
601 environmental change in the Bering Sea. J. Geophys. Res. 116, C08014.
602
603 Coachman, L.K., 1986. Circulation, water masses and fluxes on the southeastern Bering Sea
604 shelf. Cont. Shelf Res. 5, 23–108.
605
606 Coyle, K.O., Eisner, L.B., Mueter, F.J., Pinchuk, A.I., Janout, M.A., Cieciel, K.D., Farley, E.V.,
607 Andrews, A.G., 2011. Climate change in the southeastern Bering Sea: impacts on pollock
608 stocks and implications for the oscillating control hypothesis. Fish. Oceanogr. 20, 139–
609 156.
610
611 Dahlgren, K., Eriksson Wiklund, A.K., Andersson, A., 2011. The influence of autotrophy,
612 heterotrophy and temperature on pelagic food web efficiency in a brackish water system.
613 Aquat. Ecol. 45, 307-323. DOI 10.1007/s10452-011-9355-y.
614
615 Danielson, S., Eisner, L., Weingartner, T., Aagaard, K., 2011. Thermal and haline variability
616 over the central Bering Sea shelf: Seasonal and interannual perspectives Cont. Shelf Res.
617 31, 539-554. doi:10.1016/j.csr.2010.12.010.
618
619 Egge, J.K., Aksnes, D.L., 1992. Silica as regulating nutrient in phytoplankton competition.
620 Marine Ecology Progress Series. Oldendorf 83(2-3), 281-289.
621
622 Eisner, L.B., Gann, J.C., Ladd, C., Cieciel, K.D., this issue. Late summer phytoplankton biomass
623 in the eastern Bering Sea: spatial and temporal variations and factors affecting
624 chlorophyll a concentrations. Deep Sea Res II.
625
626 Eisner, L., Napp, J., Mier, K., Pinchuk, A., Andrews A., 2014. Climate-mediated changes in
627 zooplankton community structure for the eastern Bering Sea. Deep Sea Res II
628 http://dx.doi.org/10.1016/j.dsr2.2014.03.004.
629
630 Farley, E.V. Jr., Heintz, R.A., Andrews, A.G., Hurst, T.P. this issue. Size, diet, and condition of
631 age-0 Pacific cod (*Gadus macrocephalus*) during warm and cool climate states in the
632 eastern Bering Sea. Deep Sea Res II

Farley, E.V., Moss, J.H., 2009. Growth rate potential of juvenile chum salmon on the eastern Bering Sea shelf: An assessment of salmon carrying capacity. N. Pac. Anad. Fish Com. Bull. 5, 265-277

Farley, E. V., Starovoytov, A., Naydenko, S., Heintz, R., Trudel, M., Guthrie, C., Guyon, J. R., 2011. Implications of a warming eastern Bering Sea for Bristol Bay sockeye salmon. ICES Journal of Marine Science 68(6), 1138-1146.

Fu, G., Baith, K. S., McClain, C. R. "SeaDAS: The SeaWiFS Data Analysis System", Proceedings of "The 4th Pacific Ocean Remote Sensing Conference", Qingdao, China, July 28-31, 1998. 73-79.

Gordon, H. R., Wang, M. 1994. Retrieval of water-leaving radiance and aerosol optical thickness over the oceans with SeaWiFS: a preliminary algorithm. Appl. Opt. 33, 443-452.

Granger, J., Prokopenko, M.G., Mordy, C.W., Sigman, D.M., 2013. The proportion of remineralized nitrate on the ice-covered eastern Bering Sea shelf evidenced from the oxygen isotope ratio of nitrate. Global Biogeochemical Cycles, 24, 962-971.

Hama, T., Miyasaki, T., Ogawa, Y., Iwakuma, T., Takahashi, M., Otsuki, A., Ichimura, S., 1983. Measurement of photosynthetic production of a marine phytoplankton population using a 13C stable isotope. Mar. Biol. 73, 31-36.

Heintz, R.A., Siddon, E.C., Farley E.V., Napp, J.M., 2013. Correlation between recruitment and fall condition of age-0 pollock (*Theragra chalcogramma*) from the eastern Bering Sea under varying climate conditions. Deep Sea Res II 94, 150-156.

Holling, C.S. 1959. The components of predation as revealed by a study of small mammal predation of the European Pine Sawfly. *Canadian Entomologist* 91, 293-320

Hunt, G.L. Jr., Coyle, K.O., Eisner, L.B., Farley, E.V., Heintz, R., Mueter, F., Napp, J.M., Overland, J.E., Ressler, P.H., Salo, S., Stabeno, P.J., 2011. Climate impacts on eastern Bering Sea food webs: A synthesis of new data and an assessment of the Oscillating Control Hypothesis. ICES J. Mar. Sci. 68, 1230-1243.

Ianelli, J.N., Honkalehto, T., Barbeaux, S., and Kotwicki, S., 2014. Assessment of Alaska pollock stock in the Eastern Bering Sea. In: Stock Assessment and Fishery Evaluation Report for the Groundfish Resources of the Bering Sea/Aleutian Islands Regions. Anchorage: North Pacific Fisheries Management Council, pp. 55–1562.

JGOFS, 1994. Protocols for the joint global ocean flux study (JGOFS) core measurements. IOC, Scientific Committee on Oceanic Research. Manuals and Guides. Vol. 29, Paris, France, UNESCO Publishing, 170 p.

678 Kachel, N.B., Hunt Jr., G.L., Salo, S.A., Schumacher, J.D., Stabeno, P.J., Whitledge, T.E., 2002.
679 Characteristics and variability of the inner front of the southeastern Bering Sea. Deep Sea
680 Res. II 49 (26), 5889–5909.
681
682 Ladd, C., Stabeno, P.J., 2012. Stratification on the Eastern Bering Sea shelf revisited. Deep Sea
683 Res. II 65-70, 72-83.
684
685 Lomas, M.W., Moran, S.B., Casey, J.R., Bell, D.W., Tiahlo, M., Whitefield, J., Kelly, R.P.,
686 Mathis, J.T., Cokelet, E.D., 2012. Spatial and seasonal variability of primary production
687 on the eastern Bering Sea shelf. Deep Sea Res. II 65-70, 126-140.
688
689 MacKenzie, B.R., Miller, T.J., Cyr, S., Leggett, W.C., 1994. Evidence for a dome-shaped
690 relationship between turbulence and larval fish ingestion rates. Limnol. Oceanogr. 39(8),
691 1790-1799.
692
693 Moran, S.B., Lomas, M.W., Kelly, R.P., Gradinger, R., Iken, K., Mathis, J.T., 2012. Seasonal
694 succession of net primary productivity, particulate organic carbon export, and autotrophic
695 community composition in the eastern Bering Sea. Deep Sea Res II 65-70, 84-97.
696
697 Mordy, C.W., Cokelet, E.D., Ladd, C., Menzia, F.A., Proctor, P., Stabeno, P.J., Wisegarver, E.,
698 2012. Net community production on the middle shelf of the Eastern Bering Sea. Deep-
699 Sea Res. II, 65–70, 110–125.
700
701 Moss, J.H., Farley, E.V. Jr, Feldmann, A.M., Ianelli, J.N., 2009. Spatial distribution, energetic
702 status, and food habits of eastern Bering Sea age-0 walleye pollock. Transactions of the
703 American Fisheries Society 138(3), 497-505.
704
705 Mueter, F.J., Bond, N.A., Ianelli, J.N., Hollowed, A.B., 2011. Expected declines in recruitment
706 of walleye pollock (Theragra chalcogramma) in the eastern Bering Sea under future
707 climate change. ICES Journal of Marine Science 68(6), 1284-1296.
708
709 Mueter, F.J., Ladd, C., Palmer, M.C., Norcross, B.L., 2006. Bottom-up and top-down controls of
710 walleye pollock (*Theragra chalcogramma*) on the eastern Bering Sea shelf. Prog.
711 Oceanogr. 62, 152-183.
712
713 O'Reilly, J.E., and co-authors, 2000. Ocean color chlorophyll a algorithms for SeaWiFS, OC2,
714 and OC4: Version 4. In: SeaWiFS Postlaunch Technical Report Series, edited by Hooker,
715 S.B and Firestone, E.R. Volume 11, SeaWiFS Postlaunch Calibration and Validation
716 Analyses, Part 3. NASA, Goddard Space Flight Center, Greenbelt, Maryland. 9-23.
717
718 Ortiz, I., Wiese, F., Greig, A., 2012. Marine Regions Boundary Data for the Bering Sea Shelf
719 and Slope. UCAR/NCAR - Earth Observing Laboratory/Computing, Data, and Software
720 Facility. Dataset. doi:10.5065/D6DF6P6C
721
722 Parsons, T.R., Maita, Y., Lalli, C.M., 1984. A Manual of Chemical and Biological Methods for
723 Seawater Analysis. Pergamon Press, Oxford, England, 173 pp.

R Core Team, 2013. R: A language and environment for statistical computing. R Foundation for Statistical computing, Vienna, Austria. ISBN 3-900051-07-0, URL http://www.R-project.org/.

Rho, T., Whitledge, T.E., 2007. Characteristics of seasonal and spatial variations of primary production over the southeastern Bering Sea shelf. Cont. Shelf Res. 27, 2556-2569.

Rothschild, B.J., Osborn, T.R., 1988. Small scale turbulence and plankton contact rates. J Plankton Res 10, 465-474.

Sambrotto, R.N., Niebauer, H.J., Goering, J.J., Iverson, R.L., 1986. Relationships among vertical mixing nitrate uptake and phytoplankton growth during the spring bloom in the southeast Bering Sea middle shelf. Cont. Shelf Res. 5, 161–198.

Shettle, E. P., and R. W. Fenn. 1979. Models for the Aerosols for the Lower Atmosphere and the Effects of Humidity Variations on Their Optical Properties. AFGL-TR-79-0214 Environmental Research Papers No. 676.

Siddon, E.C., Heintz, R.A., Mueter F.J., 2013. Conceptual model of energy allocation in Walleye Pollock (*Theragra chalcogramma*) from larvae to age-1 in the eastern Bering Sea. Deep Sea Res II 94, 140-149.

Sigler, M.F., Heintz, R.A., Hunt, G.L., Lomas, M.W., Napp, J. M., Stabeno, P., this issue. A mid-trophic view of subarctic productivity: lipid storage, location matters and historical context. Deep-Sea Res. II.

Sigler, M.F., Stabeno, P.J., Eisner, L.B., Napp, J.M., Mueter, F.J., .2014. Spring and fall phytoplankton blooms in a productive subarctic ecosystem, the eastern Bering Sea, during 1995–2011. Deep Sea Res II 109, 71-83.

Smart, T.I., Siddon, E.C., Duffy-Anderson, J.T., 2013. Vertical distributions of the early life stages of walleye pollock (Theragra chalcogramma) in the Southeastern Bering Sea. Deep-Sea Research II 94, 201-210.

Stabeno, P.J., Danielson, S., Kachel, D., Kachel, N.B., Mordy, C.W., this issue. Currents and transport on the Eastern Bering Sea shelf. Deep-Sea Res. II.

Stabeno, P.J., Kachel, N.B., Moore, S.E., Napp, J.M., Sigler, M., Yamaguchi, A., Zerbini, A.N., 2012. Comparison of warm and cold years on the southeastern Bering Sea shelf and some implications for the ecosystem. Deep Sea Res. II 65-70, 31-45.

Stabeno, P.J., Napp, J., Mordy, C., Whitledge, T., 2010. Factors influencing physical structure and lower trophic levels of the eastern Bering Sea shelf in 2005: sea ice, tides and winds. Prog. Oceanogr. 85 (3-4), 180–196.

770 Sverdrup, H.U., 1953. On conditions for the vernal blooming of phytoplankton. J. Cons. Cons.
771 Int. Explor. Mer 18, 287-295.
772
773 Vargas, C.A., Martinez, R.A., Escribano, R., Lagos, N.A., 2010. Journal of the Marine
774 Biological Association of the United Kingdom, 2010, 90(6), 1189–1201.
775 doi:10.1017/S0025315409990804
776
777 Wiese, F.K., Wiseman, W.J., van Pelt, T.I., 2012. Bering Sea linkages. Deep Sea Res. II 65-70,
778 2-5.
779
780 Wood S.N. 2006. Generalized linear models: an introduction with R. Boca Raton, FL, USA.
781 Chapman and Hall/CRC. 392 p.
782
783 Wyatt, S.N., Crawford, D.W., Wrohan, A., Varela, D.E. 2013. Distribution and composition of
784 suspended biogenic particles in surface waters across Subarctic and Arctic Seas, J.
785 Geophys. Res., 118, DOI: 10.1002/2013JC009214
786
787 Zador, S., 2014. Ecosystem Considerations 2014, Stock Assessment and Fishery Evaluation
788 Report, North Pacific Fisheries Management Council, 605 W 4th Ave, Suite 306,
789 Anchorage, AK 99501.
790
791

Tables

Table 1. Average mixed layer depth (m), surface temperature (mean above the mixed layer depth, ºC), bottom temperature (mean below the mixed layer depth, ºC), and start and end dates for sampling in Region 3 during BASIS late summer/early fall surveys. Minimum and maximum values are bolded for each category.

Year	Mixed Layer Depth	Temp surface	Temp bottom	Sampling start	Sampling end
2006	19.2	9.85	**4.13**	20-Aug	**3-Sep**
2007	**17.4**	**10.85**	2.86	**16-Aug**	13-Sep
2008	19.7	8.85	2.86	**12-Sep**	26-Sep
2009	19.2	**7.81**	2.55	4-Sep	**27-Sep**
2010	18.1	8.49	2.2	19-Aug	16-Sep
2011	**21.5**	8.55	3.94	24-Aug	19-Sep
2012	19.1	8.58	**1.99**	24-Aug	13-Sep

Table 2. *P*-values (Kruskal-Wallis rank sum test, α = 0.05) to investigate interannual differences in surface PP (absolute uptake and uptake normalized to Chl *a* and to PAR), surface silicic acid, surface Chl *a*, and surface >10 µm Chl *a* for 2006-2012, unless otherwise noted. Data are from PP station locations (Fig. 1) with the exception of 2008 and 2012, which are from Region 3, on the southeast middle shelf. The last column shows year pairs with significant differences ($P < 0.05$) using Student Newman-Keuls test for log transformed surface silicic acid, surface Chl *a* and >10 µm Chl *a*; see Appendix Tables A1, A2, A3 for details. N/A indicates a lack of data.

PP parameter	**Factor**	**Test**	**P-Value**	**Year pairs with significant differences**
Absolute Uptake	Year (06-11), exclude 08	Kruskal-Wallis	**0.008**	**N/A**
Uptake normalized to Chl *a*	Year (06-11) exclude 08	Kruskal-Wallis	**0.02**	**N/A**
Uptake normalized to Chl *a* and PAR	Year (07, 09, 10)	Kruskal-Wallis	**0.009**	**N/A**
Log transformed Silicic acid	Year (06-12)	One way ANOVA	**<< 0.01**	**2007 < all years**
Log transformed Chl *a*	Year (06-12)	One way ANOVA	**0.012**	**2007<2009, 2011**
Log transformed >10 µm Chl *a*	Year (06-12)	One way ANOVA	**<< 0.01**	**2007<2009** **2008<2009** **2012<2006, 2009, 2011**

Table 3. MODIS satellite ocean color data for Region 3 Chl *a* depicting the spring and autumn bloom peak months, and the mean Chl *a* (mg m^{-3}) and standard error (SE) for spring (March-May), summer (June-Aug) and March-August, 2006-2012. Grand mean for 2006-2012 shown for comparison. ANOVA *P*-values indicate no significant differences among years.

Year	Spring Peak	Autumn Peak	Mar-May Chl *a* Mean ±SE	Jun-Aug Chl *a* Mean ±SE	Sep-Oct Chl *a* Mean ±SE	Mar-Aug Chl *a* Mean ±SE
2006	Jun	Sept	1.30 ±0.21	1.54 ±0.75	1.29 ±0.07	1.22 ±0.33
2007	Apr	Sept	1.84 ±0.73	0.86 ±0.11	1.24 ±0.24	1.16 ±0.37
2008	May	Sept	1.35 ±0.44	0.75 ±0.15	1.32 ±0.31	0.90 ±0.23
2009	May	Sept	1.98 ±0.92	1.20 ±0.23	1.84 ±0.08	1.36 ±0.43
2010	May	Sept	4.51 ±1.94	0.99 ±0.26	1.61 ±0.16	2.36 ±1.09
2011	May	Sept	2.00 ±0.74	1.13 ±0.17	1.40 ±0.00	1.34 ±0.36
2012	Apr	Oct	3.95 ±2.15	0.76 ±0.11	1.32 ±0.20	2.02 ±1.11
All years Grand mean			2.42	1.03	1.43	1.48
ANOVA P-value			$P > 0.4$	$P > 0.6$	$P > 0.3$	$P > 0.6$

817 Table 4. Mooring 2 date and magnitude (Chl *a*, mg m^{-3}) of the spring bloom maximum (Max Chl
818 *a*) from surface Chl *a* fluorescence data (reproduced from Sigler et al., 2014) and date and
819 magnitude of post bloom surface silicic acid (Si, µM) including, mean, standard deviation
820 (stdev), number of stations (N) for 2006-2011. N/A indicates a lack of data.

Year	Date Max Chl *a*	Conc. Max Chl *a*	Date Post-bloom Si	Mean Post-bloom Si	St dev Post-bloom Si	N Post- bloom Si
2006	14-Jun	28.1	N/A	N/A	N/A	N/A
2007	25-Apr	9.7	10-May	0.77	0.28	3
2008	2-May	20	N/A	N/A	N/A	N/A
2009	4-Jun	9.0	18-Jun	0.14	0.05	2
2010	6-May	16.1	31-May	1.17	0.91	8
2011	7-Jun	18.5	N/A	N/A	N/A	N/A

821

Table 5. Pearson's product correlation coefficients showing averages (2006-2012) for surface silicic acid ($Si(OH)_4$, µM), surface (Surf) Chl *a* (mg m^{-3}), integrated (Int) Chl *a* (mg m^{-2}) in Region 3 and age-0 pollock weight (A0W (g)) in the southeastern Bering Sea (south of 60ºN). Pearson correlation (*r*) is shown as the top number, with *P*-value below. Statistically significant values are given in bold font.

	A0W	$Si(OH)_4$	Surf Chl *a*
$Si(OH)_4$	0.558		
	0.193		
Surf Chl *a*	0.430	**0.838**	
	0.336	**0.018**	
Int Chl *a*	0.015	0.701	**0.782**
	0.974	0.079	**0.038**

Table 6. Ichthyoplankton spring survey sampling date, number of stations, May sea surface temperature, and predicted date of peak egg abundance from a generalized additive model for 2006-2010 and 2012 (see text).

Year	Dates sampled	# Stations	May SST[1] (°C)	Predicted date of peak egg abundance
2006	15 Apr – 23 Jun	126	1.29	28 Apr
2007	12 Apr – 30 Jun	80	1.22	13 May
2008	18 Feb – 28 Jun[2]	61	0.59	18 May
2009	2 Mar – 30 Jun[3]	92	1.31	9 May
2010	28 Apr – 29 Jun[4]	102	0.68	14 May
2012	29 Apr – 1 Jun	188	-0.04	30 May

[1]May sea surface temperature in the southeast Bering Sea. Data from www.beringclimate.noaa.gov.
[2]Only 3 stations sampled in February, remaining stations sampled in May and June
[3]Only 1 station sampled in March, remaining stations sampled in May and June
[4]Only 1 station sampled in April, remaining stations sampled in May and June

849 Table 7. Number of days for walleye pollock eggs to reach 50% hatching based on May sea
850 surface temperature (see Table 6). Hatching period represents the days during which all eggs are
851 expected to hatch based on the days to 50% hatch. Estimated hatching dates are based on eggs
852 being fertilized on the date of peak egg abundance shown in Table 6, and were calculated from
853 that date and the days of the hatching period.

Year	Days to 50% hatch	Hatching period (days)	Estimated hatching dates
2006	32	26.5 – 37.5	25 May – 5 June
2007	32	26.5 – 37.5	9 June – 20 June
2008	36	30.5 – 41.5	18 June – 29 June
2009	32	26.5 – 37.5	5 June – 16 June
2010	35	29.5 – 40.	13 June – 24 June
2012	39	33.5 – 44.5	3 July – 14 July

854

855

Table 8. Mean standard length (SL, mm) and standard error (SE) of walleye pollock larvae sampled from the Pribilof Islands spawning area of the south EBS used for size comparisons among the years 2007, 2009, 2010, and 2012.

Year	Sampling Date	No. Stations	No. Larvae[a]	Mean SL ± SE[b]
2007	9 – 14 May	28	734	4.87 ± 0.03
2009	8 – 10 May	8	34	4.46 ± 0.09*
2010	13 – 16 May	21	275	4.31 ± 0.04*
2012	25 – 31 May	53	1959	4.84 ± 0.02

[a]number of larvae measured
[b]mean standard length ± standard error
*indicates sizes that were significantly different ($P < 0.05$) from 2007

865 **Figure captions:**

866 Figure 1. Primary production experiment station locations in the southeastern Bering Sea (south
867 of 60 ºN), labeled by year, overlain with Bering Sea Project Regions (grey lines). Some years
868 have overlapping locations. Depth contours are every 50 m bathymetry (thin black lines).

869 Figure 2. Box and whisker plots depicting the median (solid horizontal line), mean values (circle
870 with cross), and extremes (whiskers) of surface (A) absolute PP uptake (mg C m^{-3} hr^{-1}), (B)
871 silicic acid (Si) concentrations (µM), (C) Chl *a* concentrations (mg m^{-3}), and (D) >10 µm Chl *a*
872 concentrations (mg m^{-3}). Data are from primary production station locations (Fig. 1) with the
873 exception of 2008 and 2012, which are from Region 3, on the southeast middle shelf. Asterisks
874 indicate outliers from 95% CI. Outliers for 2007 in panels A, B, and C are from the same date
875 and location near the Pribilof Islands (57.5°N, 168.77°W). The number of samples for each year
876 is shown along x-axis.

877 Figure 3. Line graph of monthly mean MODIS satellite Chl *a* (mg m^{-3}) data (Apr-Oct) for years
878 2006-2012 for Region 3. *Intended for color reproduction on the Web and in print.*

879 Figure 4. (A) Surface silicic acid (Si, µM), and (B) surface DIN (N): Si (M: M) for the eastern
880 Bering Sea shelf during mid-August to early October 2007. The oval highlights Region 3.
881 *Intended for color reproduction on the Web and in print.*

882 Figure 5. Interannual variability of (A) normalized surface silicic acid (Si) and normalized
883 surface Chl *a*, (B) normalized silicic acid (Si) and normalized mean weights of age-0 pollock
884 (weight), and (C) mean age-0 pollock weights (A0W, g) as a function of surface silicic acid (Si,
885 µM). Silicic acid and Chl *a* data are from Region 3 while age-0 pollock weights are from all
886 stations in the southeastern Bering Sea.

887 Figure 6. Box and whisker plot of late summer 30-60 m silicic acid ((Si) SiO_4 µM)
888 concentrations (below the pycnocline) for Region 3. The only significantly different year was
889 2011 ($P < 0.05$, ANOVA).

890 Figure 7. Regression of surface PP (mg C m^{-3} h^{-1} vs. integrated PP (mg C m^{-2} h^{-1} from stations in
891 the southeastern Bering Sea (Fig 1; $R^2 = 0.70$, $P < 0.001$).

892 Figure 8. Box and whisker plots of age-0 pollock weight (A0W, g) showing medians, means, and
893 extremes for the southeastern Bering Sea as in Fig. 2.

894 Figure 9. Age-0 pollock diet data for 2006-2012 from the southeastern Bering Sea. Percentages
895 in pie charts are listed for those species that make up proportionally 20% or more wet weight in
896 any given year. *Intended for color reproduction on the Web and in print.*

897 Figure 10. The number of age-1 recruits (overwinter survivors from age-0, y-axis) per unit
898 biomass of female spawners as a function of the average energy content (kJ per fish) of age-0
899 pollock in the southeastern Bering Sea (x-axis, $R^2 = 0.58$). Open circles show warm years in the
900 southeastern Bering Sea, filled circles are cool years and the gray symbol was a transition year.
901 Numbers above the symbols represent the year for age-0 pollock. The year 2008 was omitted due to
902 a reduced sample grid.

903

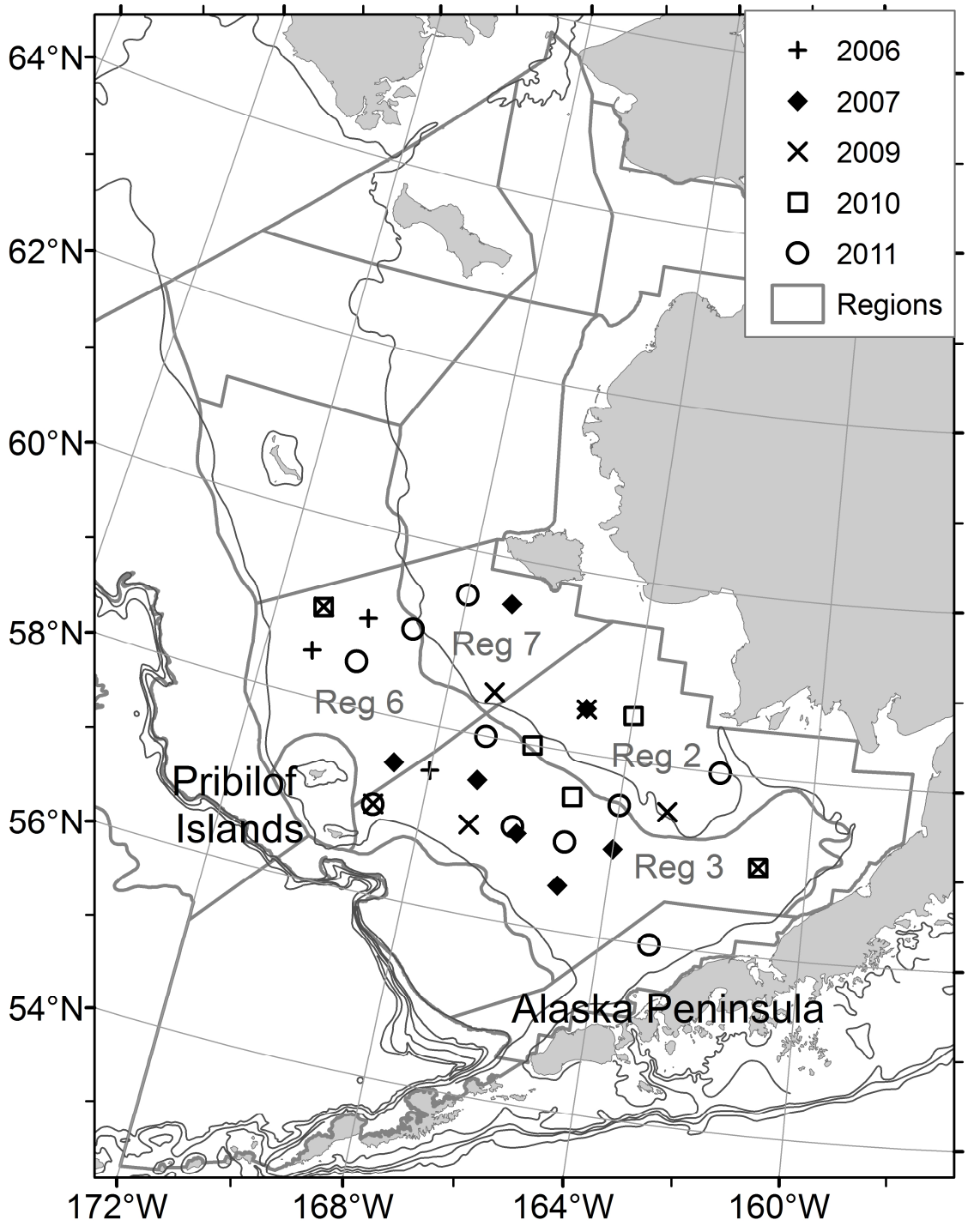

904

905 Figure 1.

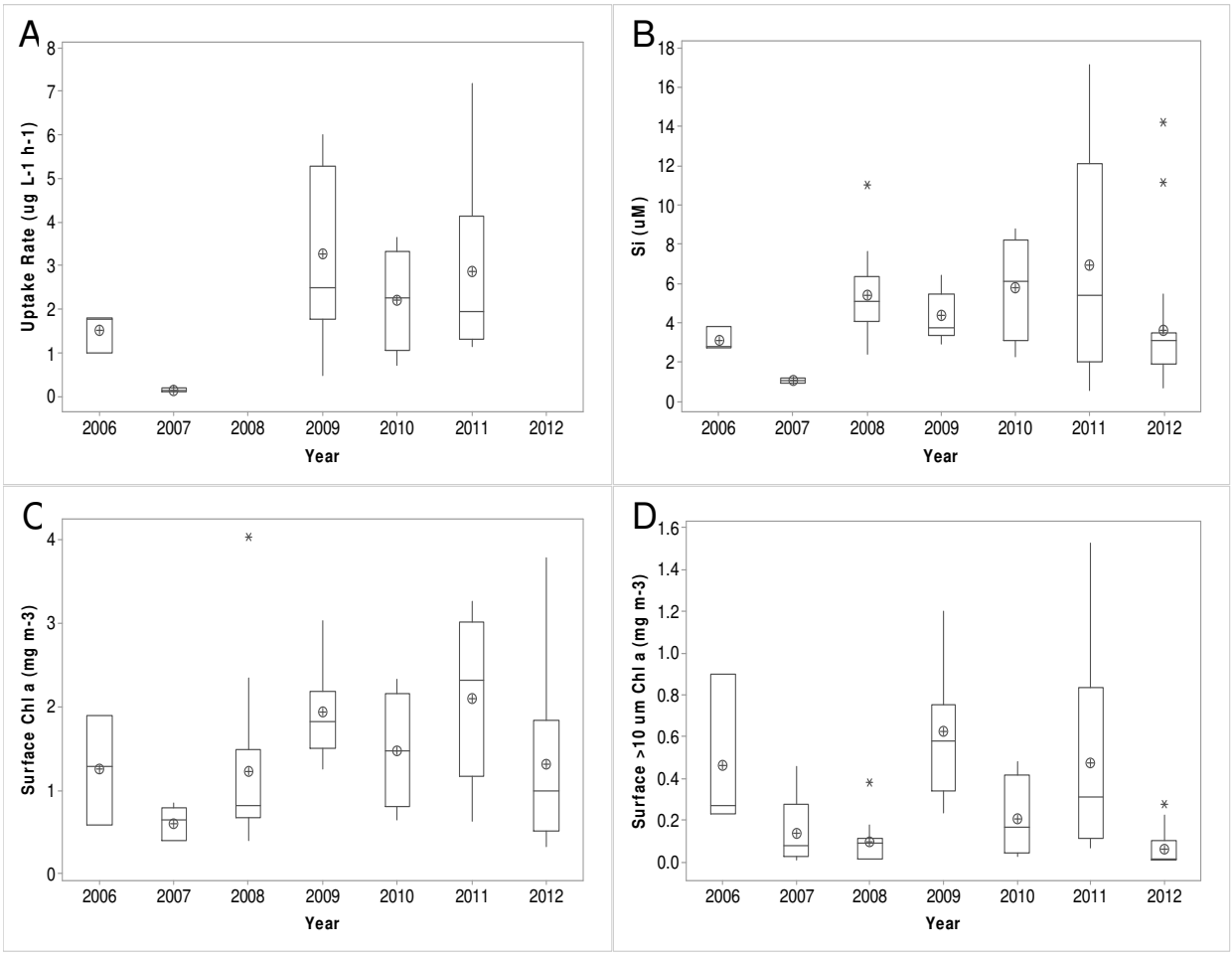
A
Uptake Rate (ug L-1 h-1)
0
1
2
3
4
5
6
7
8
2006
2007
2008
2009
2010
2011
2012
Year
B
Si (uM)
0
2
4
6
8
10
12
14
16
18
2006
2007
2008
2009
2010
2011
2012
Year
C
Surface Chl a (mg m-3)
0
1
2
3
4
2006
2007
2008
2009
2010
2011
2012
Year
D
Surface >10 um Chl a (mg m-3)
0.0
0.2
0.4
0.6
0.8
1.0
1.2
1.4
1.6
2006
2007
2008
2009
2010
2011
2012
Year

Figure 2.

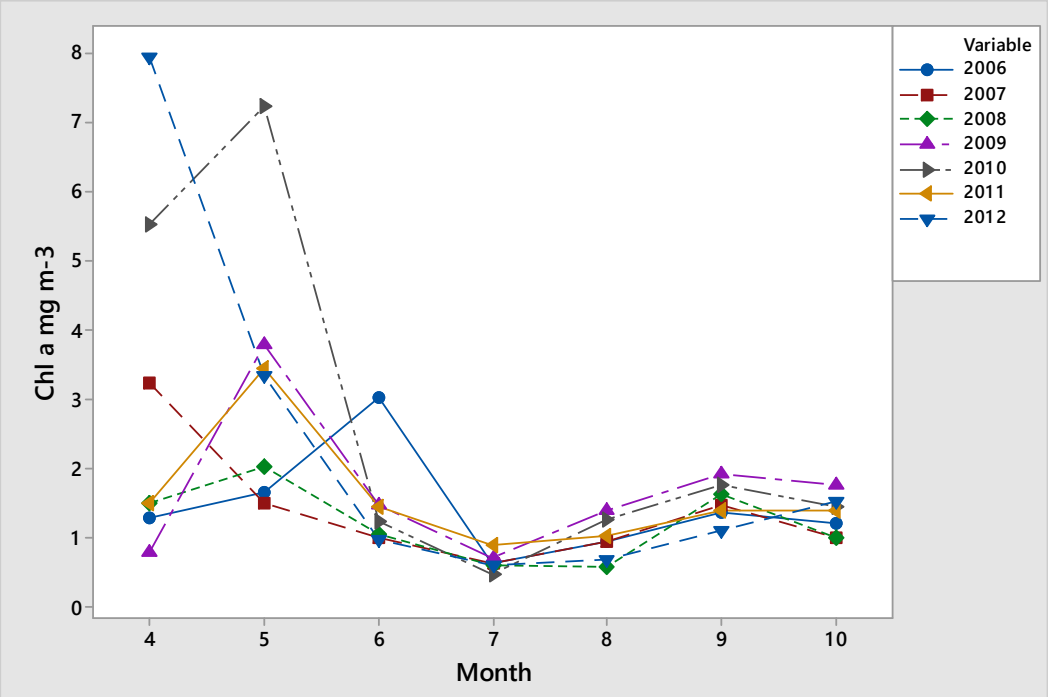
Chl a mg m-3
Month
Variable
2006
2007
2008
2009
2010
2011
2012
0
1
2
3
4
5
6
7
8
4
5
6
7
8
9
10

Figure 3.

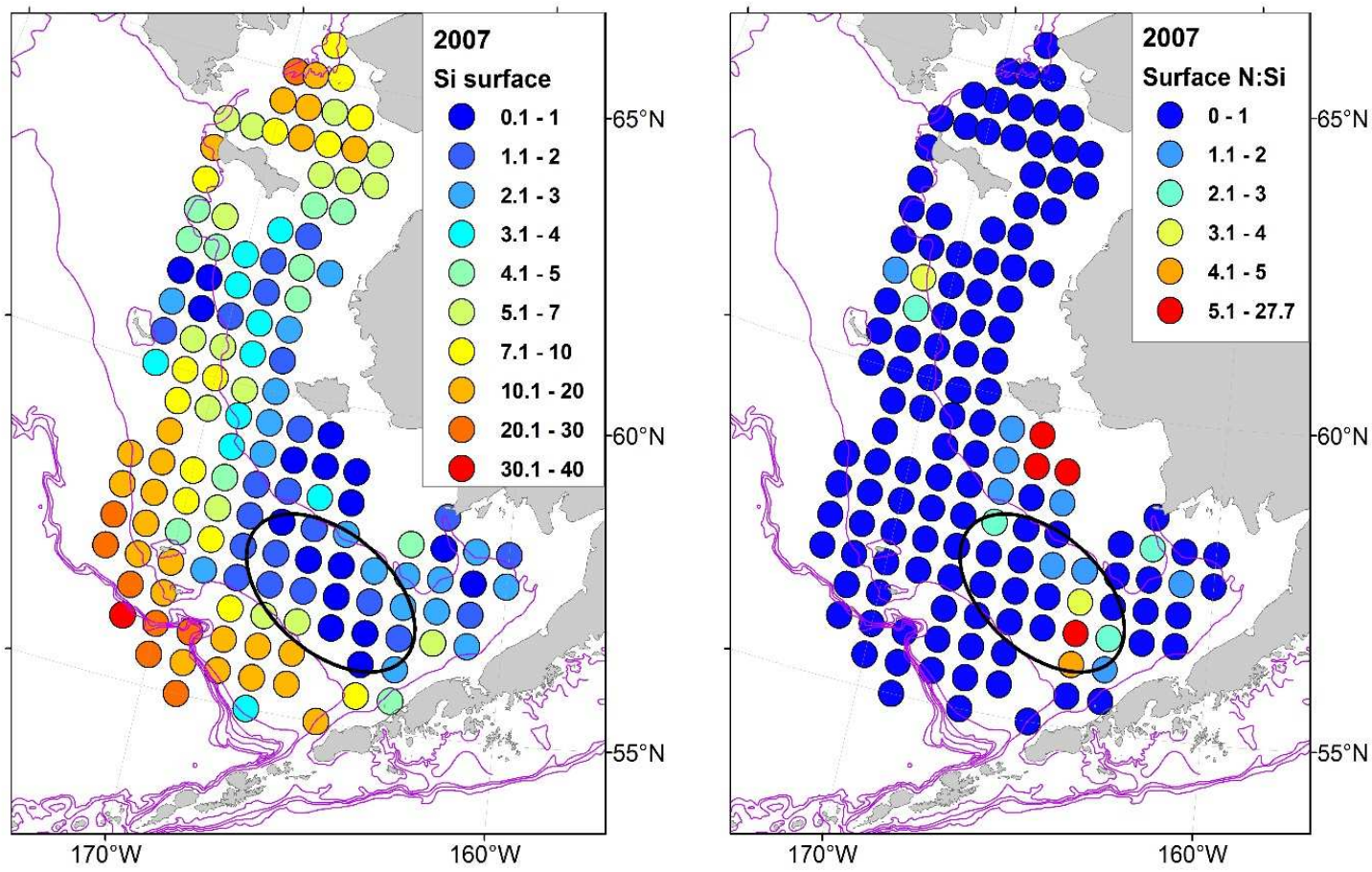

922 Figure 4.

923

924

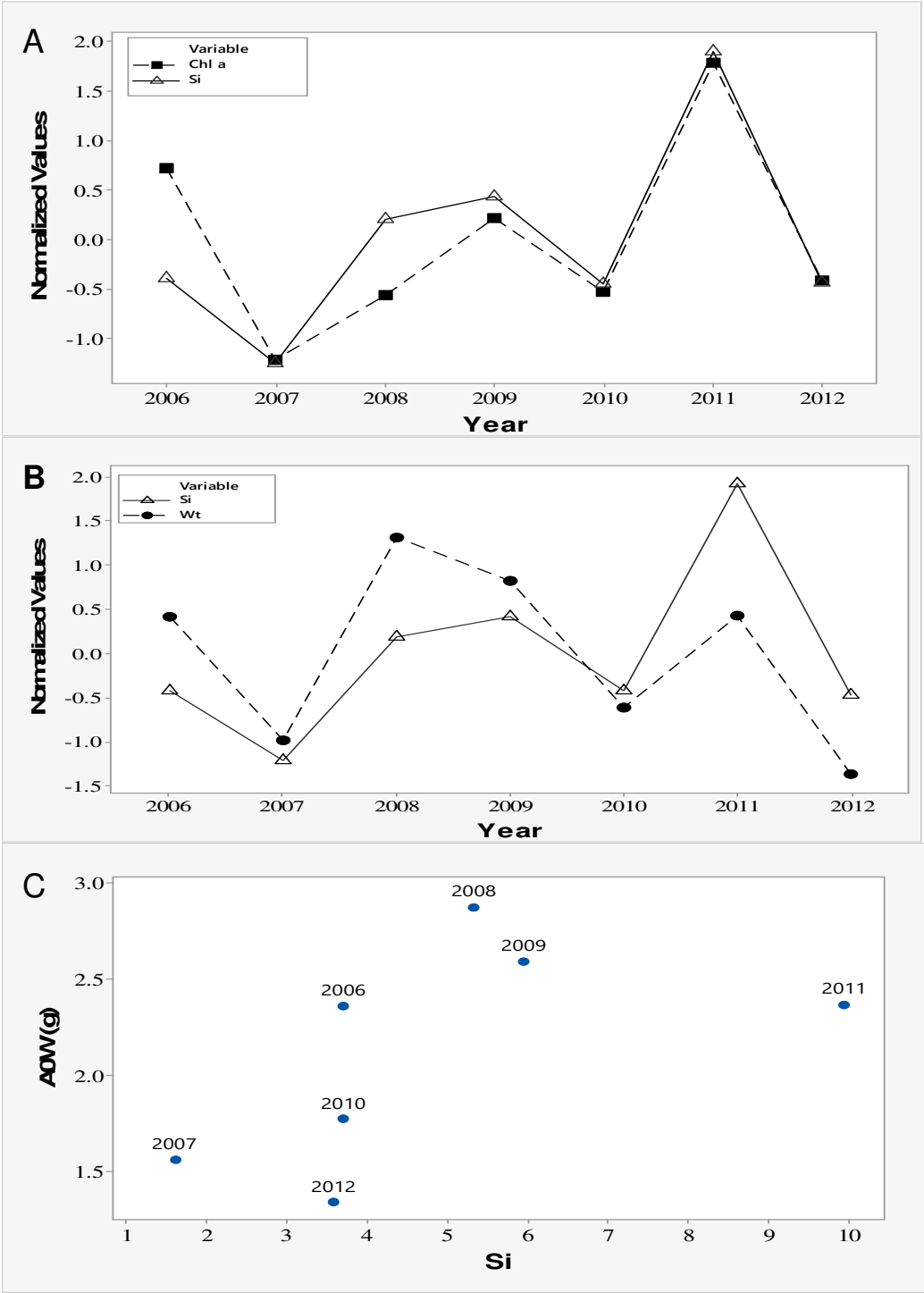
A
Variable
Chl a
Si
Normalized Values
2.0
1.5
1.0
0.5
0.0
-0.5
-1.0
2006
2007
2008
2009
2010
2011
2012
Year
B
Variable
Si
Wt
Normalized Values
2.0
1.5
1.0
0.5
0.0
-0.5
-1.0
-1.5
2006
2007
2008
2009
2010
2011
2012
Year
C
AGW(g)
3.0
2.5
2.0
1.5
2008
2009
2006
2011
2010
2007
2012
1
2
3
4
5
6
7
8
9
10
Si

Figure 5

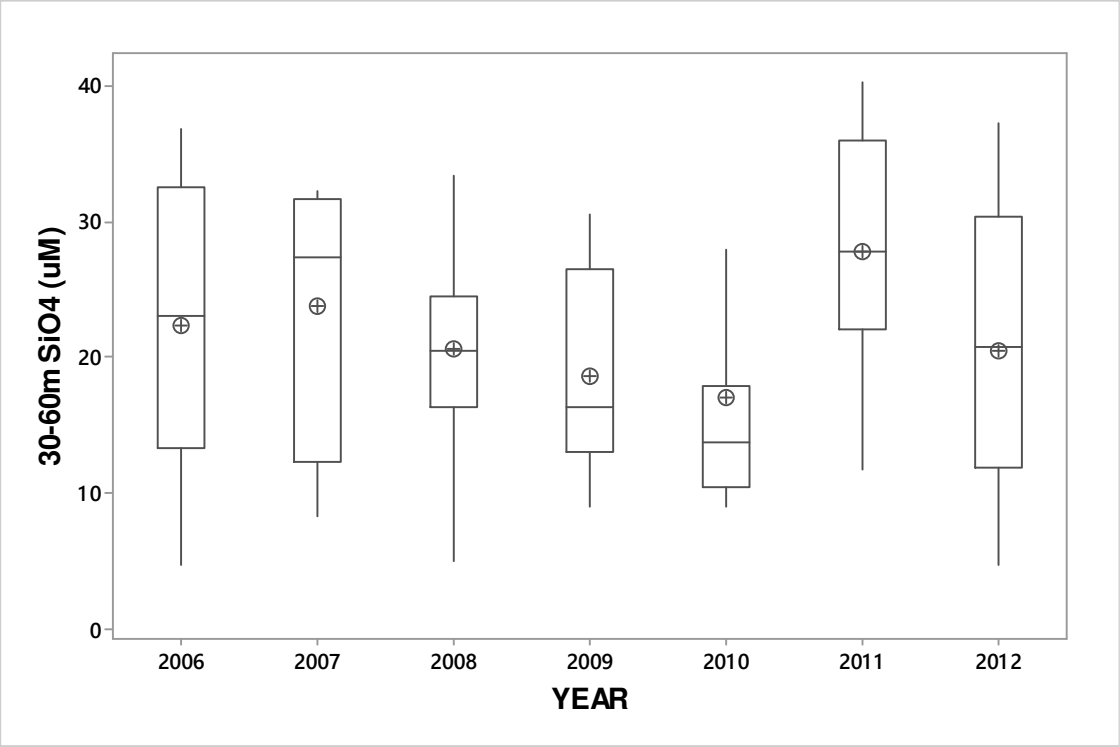

945

946 Figure 6.

947

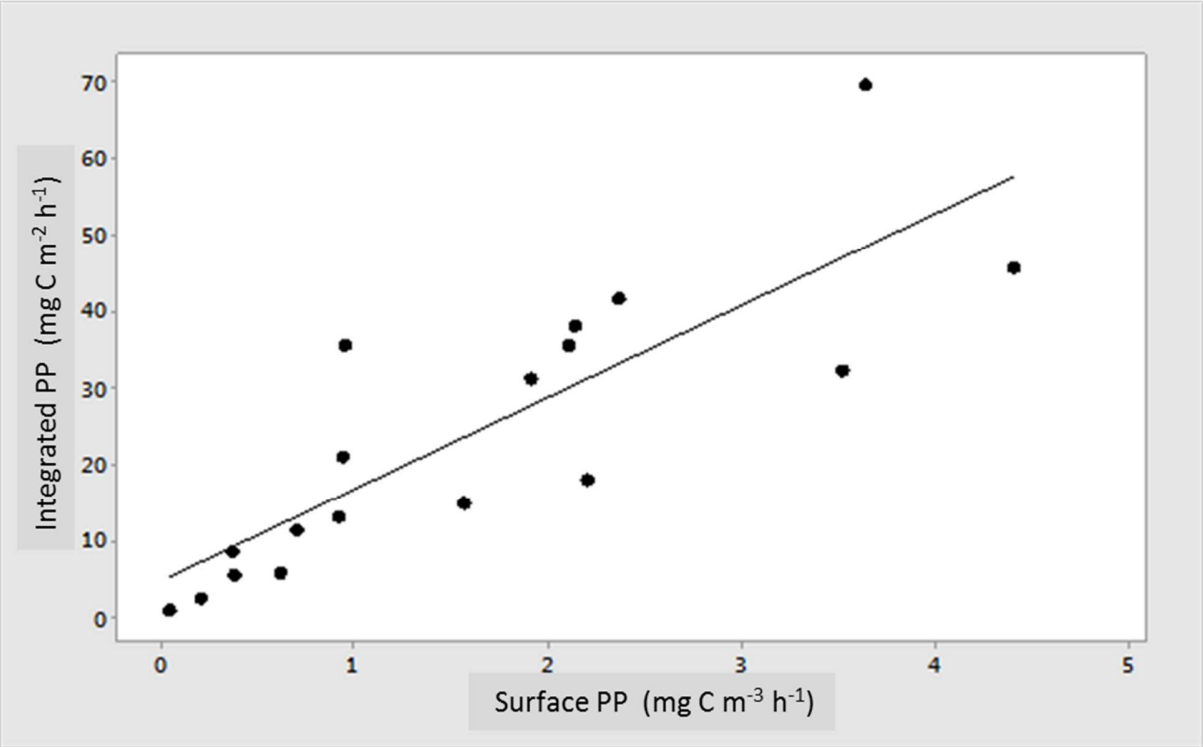
Integrated PP (mg C m-2 h-1)
70
60
50
40
30
20
10
0
0
1
2
3
4
5
Surface PP (mg C m-3 h-1)

Figure 7.

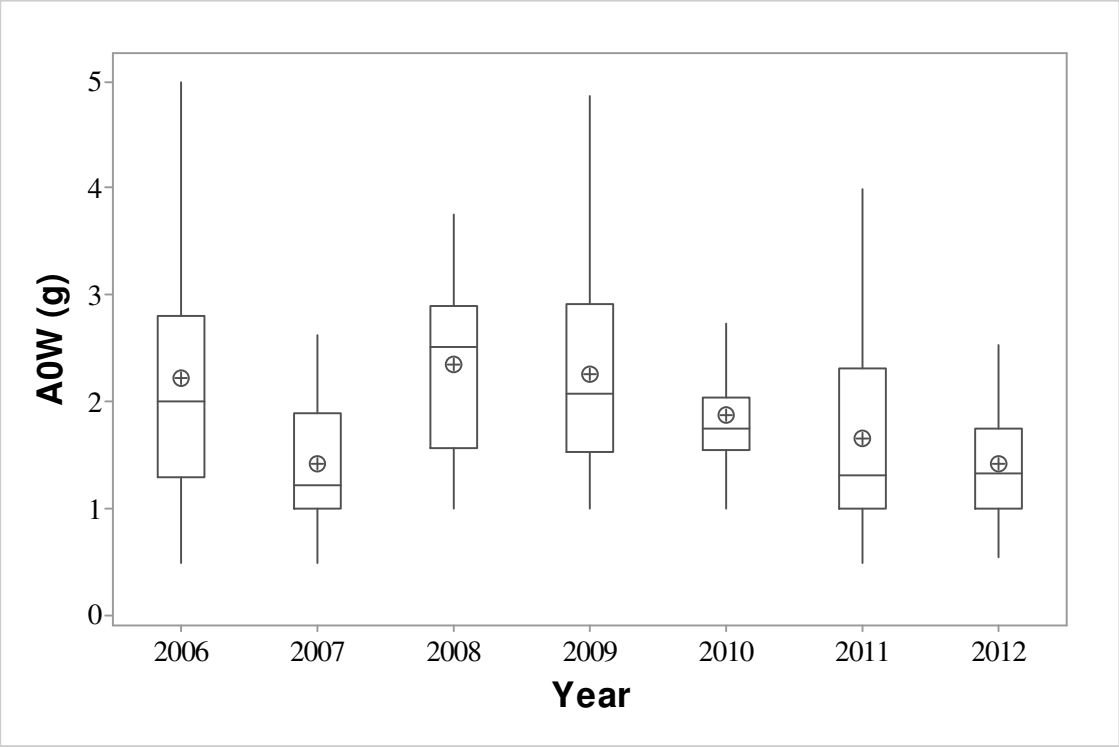

Figure 8.

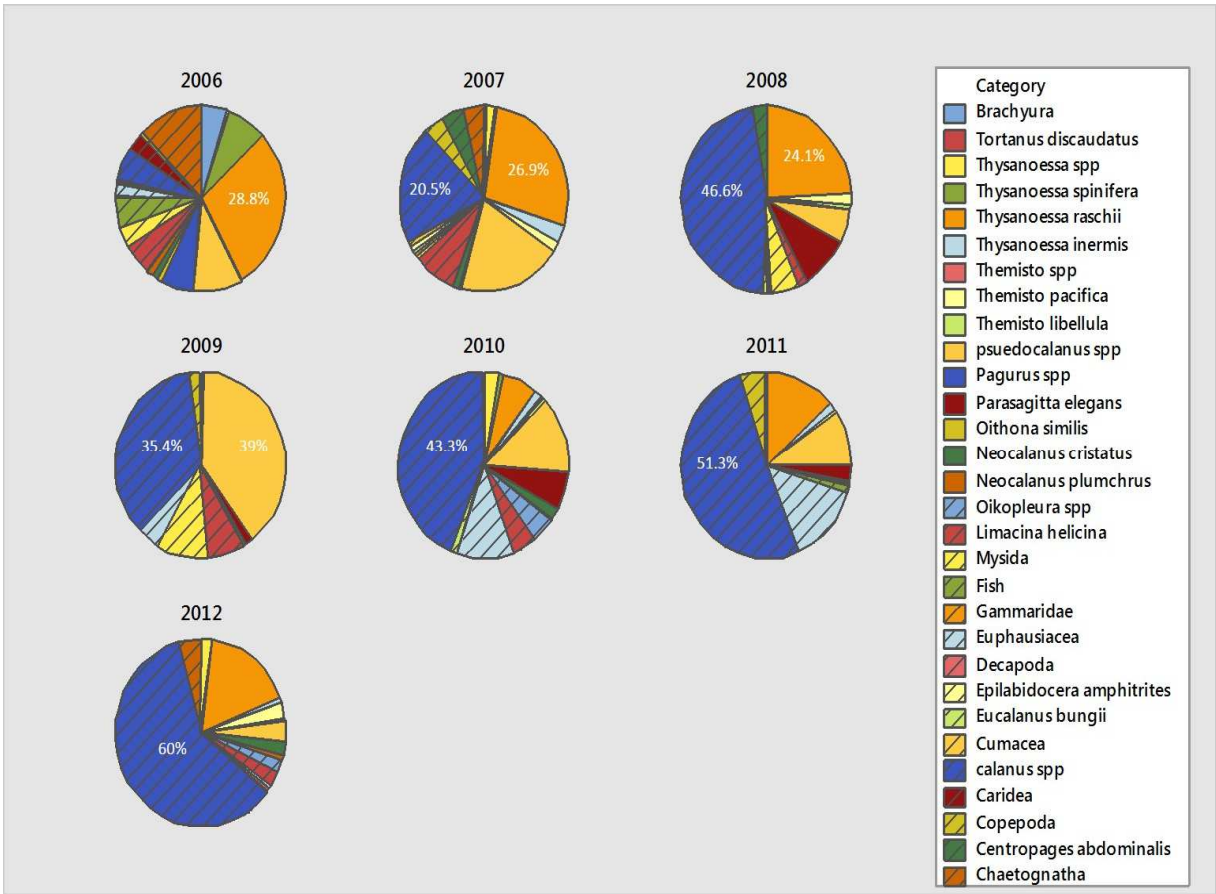

953

954 Figure 9.

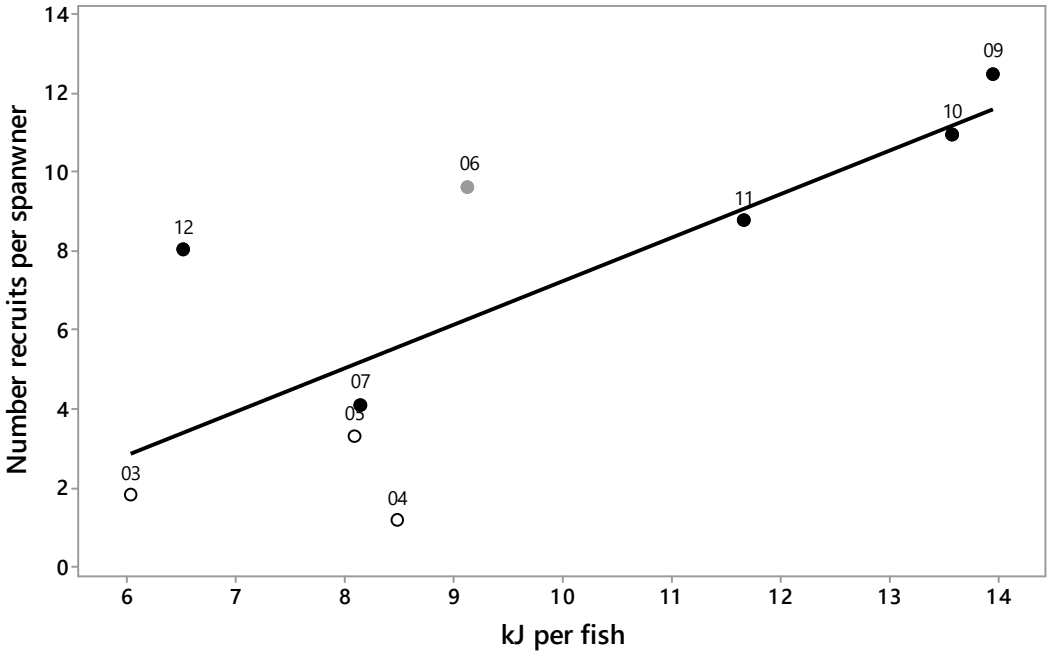

955 Figure 10.